Journal Name

ARTICLE TYPE

Deeply investigating the surface state of graphene quantum dots

Shoujun Zhu,[a] Jieren Shao,[a] Yubin Song,[a] Xiaohuan Zhao,[a] Jianglin Du,[b] Lei Wang,[b] Haiyu Wang,[b] Kai Zhang,[a] Junhu Zhang[a] and Bai Yang*[a]

Abstract. A universal route to GQDs is developed based on "solution phase-based scissor" methods. The PL center of the GQDs is systematically studied and is proved to be the surface state, which is formed by the hybridization structure of edge groups and the connected partial graphene core. Through experiment and analysis, it preliminarily proves the efficient edge groups for green emission are mainly carboxyl, 10 carbonyl as well as amide. It is illuminated by the following three cases: one is that the PL of GQDs is enhanced by the UV exposure, during which partial -OH of GQDs changes into carboxyl groups; secondly, the PL properties of GQDs can be further improved by one-step solvothermal treatment, in which partial carboxyl groups are changed to amide ones and the surface state of GQDs is enhanced; thirdly, the reduced m-GQDs possessed more -OH groups compared with the reduced GQDs, resulting 15 more blue PL center (the carboxyl, carbonyl and amide based green center was changed to -OH based blue center). The present work gives a very important direction to understand PL mechanism of GQDs and other related carbon based materials.

1. Introduction

A wide range of fluorescent carbon nanomaterials exhibit the 20 fascinating optical properties, which are very promising for low toxicity fluorescent materials.[1, 2] The most common carbon nanomaterials are carbon dots (CDs),[3-5] which mainly contained graphene quantum dots (GQDs), carbon nanodots (CNDs), and polymer dots (PDs).[6] GQDs, labeled as rising fluorescent carbon 25 materials, have drawn increasing attention these years.[7-9] The GQDs possess relative simple chemical structure with single layer graphene core and connected chemical groups, which could be regarded as a model system to understand the photoluminescence (PL) mechanism of the fluorescent carbon 30 materials.[10-13] Since excitons in graphene have an infinite Bohr diameter, graphene fragments of certain size will show quantum confinement effects.[14, 15] As a result, although large graphene has a non-zero bandgap and less PL on excitation,[16] this bandgap can be tuned not only by cutting the size but also by modifying 35 surface chemistry in GQDs.[17-19] Like most other fluorescent carbon materials, the GQDs were kinds of "uncertain" materials, it was very hard to figure out a reasonable PL mechanism.[6]

In this work, the famous "nano-cutting" route to GQDs was further developed and it showed universality for many kinds of 40 carbon resource.[20] The applied HNO₃/H₂SO₄ was a solution phase-based scissor, which exfoliated and cut the carbon resource, as well as modified the edge with oxygenic/nitrous groups, simultaneously (Scheme 1).[21-23] The PL center of the GQDs was suggested to be surface state, which was the 45 hybridization structure with edge groups and connected graphene core fragment.[24, 25] Furthermore, the PL properties can be improved by surface chemistry modifying through one-step solvothermal route or other oxidation/reduction approaches. The transient spectra proved that the surface state enhanced from 50 GQDs to m-GQDs due to the connected groups changed.
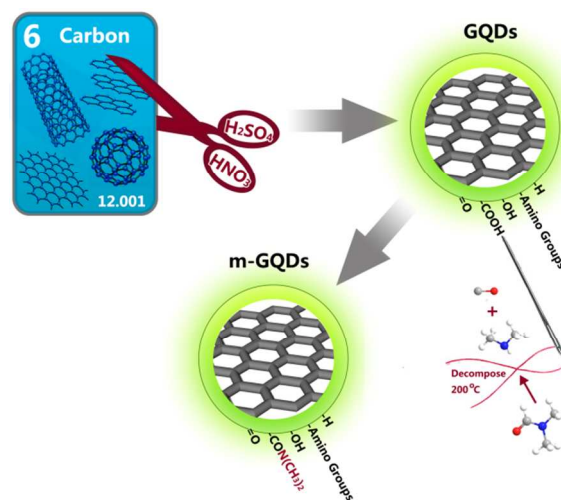
Scheme 1 The synthetic scheme for GQDs and further modification.

2. Results and discussion

The GQDs were prepared by a modified "nano-cutting" method from graphite powder and HNO_3/H_2SO_4, as shown in Scheme 1. The average diameter of the prepared GQDs was ca. 4.6 nm with crystal lattice ca. 0.21 nm, which was attributed to (100) lattice
5 plane of graphene (Fig. 1a-b).[26] The SAED pattern further supports the lamellar structure of the GQDs. From the atomic force microscope (AFM) images of the GQDs (Fig. 1c and Fig. S1), their average height was 0.8 nm, indicating that most of the GQDs are single or bi-layered.[19] In the FTIR analysis of GQDs,
10 stretching vibrations of C-OH at 3430 cm^{-1}, C-H at 2923 cm^{-1} and 2850 cm^{-1}, as well as asymmetric stretching vibrations of C-NH-C at 1126 cm^{-1}, bending vibrations of N-H at 1570 cm^{-1} and a vibrational absorption band of C=O at 1635 cm^{-1} were all observed (Fig. S2a). In addition, edge groups were also
15 investigated by XPS analysis (Fig. S2b-d). The C1s analysis revealed three different types of carbon: graphitic or aliphatic carbon (C=C/C-C), oxygenated carbon and nitrous carbon.[27] From MALDI-TOF MS spectra of GQDs (Fig. 1d), the molecular weights were mainly between 1250-2750 with a regular interval
20 (58 Da). It indicated that the neighbouring GQD differed by a "$C_2O_2H_2$" groups (Fig. 1e).[12, 28] Three kinds of "$C_2O_2H_2$" groups were listed in Fig. 1e, which was generated by the acid-assisted cutting process. The –OH was mainly produced by the cutting position through epoxy,[20] while the –COOH and carbonyl was the
25 stable oxidation state. The Fig. S3 shows the suggested chemical structure of the GQDs. Furthermore, the GQDs possess outstanding solubility (over 20 mg/mL) in aqueous solution, which will be very important for the practical applications.[10]
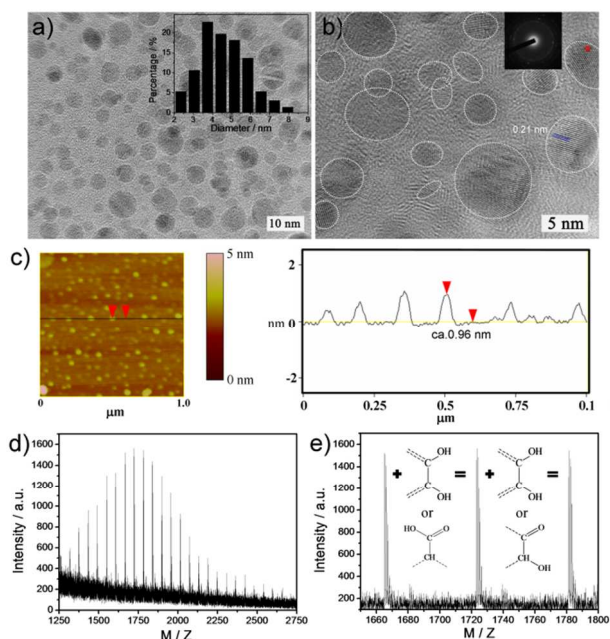
Fig. 1 a-b) TEM images of GQDs at different amplification. Inset images
30 were size distributions and selected area electron diffraction. c) The AFM image of GQDs, and the height of most of GQDs was less than 1 nm. d-e) The MALDI-TOF spectra of the GQDs.

In the UV-Vis spectra, there were obvious absorption peaks from UV to blue region in aqueous solution of GQDs (Fig. 2a),
35 which contained the π-π*, n-π* as well as surface state transition.

The π-π* is assigned to the aromatic sp^2 domains; n-π* and the surface state belonged to the nitrogen or oxygen based groups, as well as the hybrid structure of the partial carbon skeleton and edge groups.[29] In the fluorescence spectra, GQDs possess the
40 optimal excitation and emission wavelengths at ca. 468 and 525 nm, respectively, and showed green-yellow color under a hand-hold UV lamp (Fig. 2b). The surface state was induced by the hybridization structure of edge groups and connected carbon core, and the participant edge groups for green emission mainly
45 resulted from carboxyl and amide. It should be noted that the –OH based hybrid structure mainly contributed to the blue emission, or to a certain degree, enriched the electron density of the π structure; so the GQDs possessed elevated quantum yield and blue-shift emission by $NaBH_4$ reduction.[10, 12] As a result, No
50 matter which the energy level of LUMO band the electron was excited to, it finally relaxed into the energy levels of surface state, which determined the PL properties of GQDs (Fig. 2c).[30] Fortunately, the excitation-dependent PL behaviors can be applied in long wavelength for biological imaging fields, this
55 excitation-dependent PL behaviors may be induced by wide size and surface chemistry distribution,[31] excited electron relax to different energy level,[32] as well as long solvation in water (Fig. S4).[33, 34]
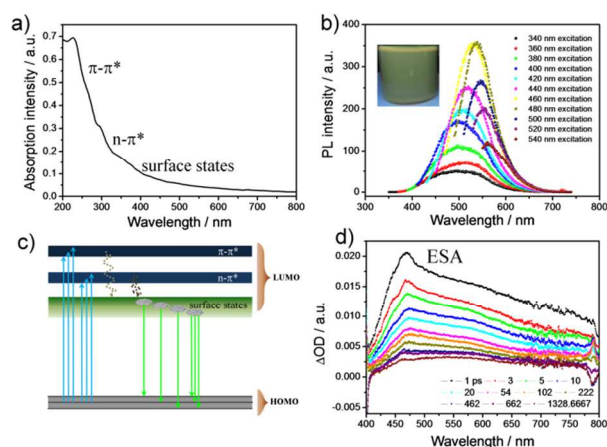
Fig. 2 The optical property of GQDs. a) UV/Vis absorption spectra of the
60 GQDs. b) The PL spectra of GQDs in aqueous solutions. Insets show photographs of GQDs in aqueous solutions under UV light. c) The surface state determined the PL of GQDs. d) TA spectra of GQDs, there was only a positive excited-state absorption (ESA).

The decay time of GQDs was ranged from 1 to 3.5 ns probed
65 from 410 to 770 nm, which contained two nanosecond components (Fig. S5a), the short τ_1 may belong to the non-radiative process while the long τ_2 belongs to the PL emission.[35] To gain more insight into the origin of the PL behavior of the GQDs, the femtosecond transient absorption (TA) spectroscopy
70 was performed (Fig. 2d and Fig. S5b-d).[36, 37] All the features in TA reflect the information about the change of photogenerated carrier populations in corresponding energy levels.[38, 39] The similar excited-state behaviors (the same excited-state absorption (ESA)) by different excitation wavelength reveal that the GQDs
75 possess very weak PL properties, which further proved that the carboxyl based surface state was relative weak PL center.

In addition, GQDs possessed high photo-stability (Fig. 3a-b), after a certain time of high power UV exposure, the PL intensity and the lifetime of GQDs increased to some degree. And it may be induced by destroying the chemical groups of non-radiative process at the edge of GQDs, which also contributed to the surface state changing of GQDs (Fig. S6).[11, 40] For example, the electron-withdrawing nitro could be destroyed by free radical in UV exposure process, while the -OH groups tend to change to carbonyl/carboxyl groups in this process; and all of these changes can enhance the surface state (green emission) of GQDs (inset of Fig. 3b).[41] It was further proved by the nanosecond components changing of the PL lifetime: the percentage of τ_1 decreased while that of τ_2 increased (Fig. 3c and Table S1).
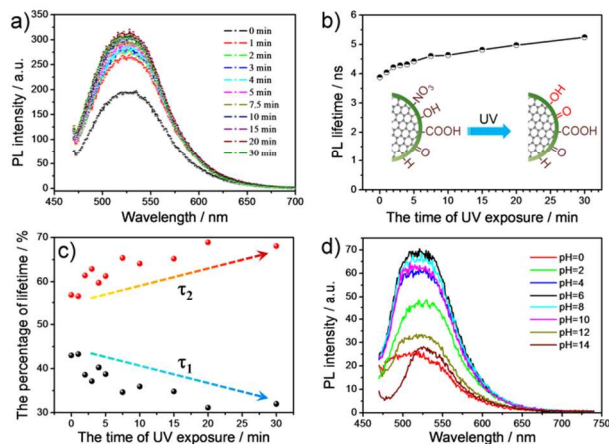

Fig. 3 a-b) The PL property and lifetime of GQDs after 2000 W UV exposure with different time. The inset was the scheme of GQDs changing after UV exposure (the oxygen based groups were suggested based on the MALDI-TOF result in Fig. 1e. c) The evolution of short and long lifetime of GQDs by UV exposure. d) The pH-dependent PL of the GQDs aqueous solution.

We further found that the GQDs exhibited the same pH-dependent PL behavior with previous CDs and solvothermally GQDs.[42] The intensities of green emission decrease in the solution of both high and low pH value (Fig. 3d). It indicated that the pH-dependent behaviors at specific ranges may contribute to the protonation/deprotonation of carboxyl groups, which affected the PL center of the green emission. In addition, the PL of the GQDs shifted to long wavelength with increasing the

concentration of GQDs aqueous solution (Fig. S7), which was induced by the accumulated excitation and emission of GQDs in the high concentration of aqueous solution.[43, 44] In a word, all of these steady/transient state experiments confirmed the common contribution of oxygen/nitrous-based groups at the edge on the emission of fluorescent carbon nanomaterials.[10]
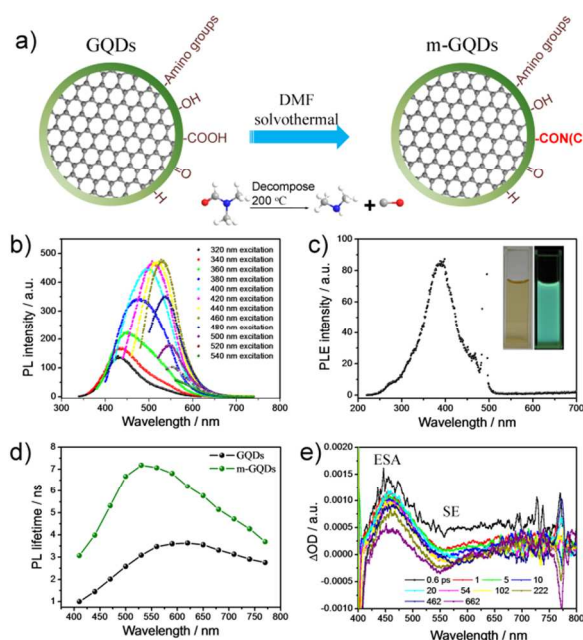
The present acid-assisted nano-cutting method was a universal approach to prepare GQDs from different carbon resources.[45] As shown in Fig. 4, Table S2 and Fig. S8-9, the GQDs prepared by different carbon resource were presented here for reference. The optimal reaction temperature was ca. 120 °C and the output was over 50%.[45] The low temperature (less than 100 °C) lead to the incomplete reaction, while the high temperature (higher than 140 °C) resulted in the low yield of GQDs due to the over oxidation (most of the carbon resource was converted into the CO_2 and H_2O).[46] The diameter of the series prepared GQDs was ca. 1-10 nm with crystal lattice from 0.21-0.29 nm, most of which is attributed to (100) or (020) lattice plane of graphite (Fig. 4). The quantum yields of the prepared GQDs were always lower than 1%, and the average lifetime was 2-3.5 ns. All the GQDs possessed the optimal emission at ca. 525 nm with green-yellow color, but the apparent photographs obtained by the UV light excitation were from green to yellow color. In addition, all the prepared GQDs possessed negative charge due to the modification of oxygen-based groups.
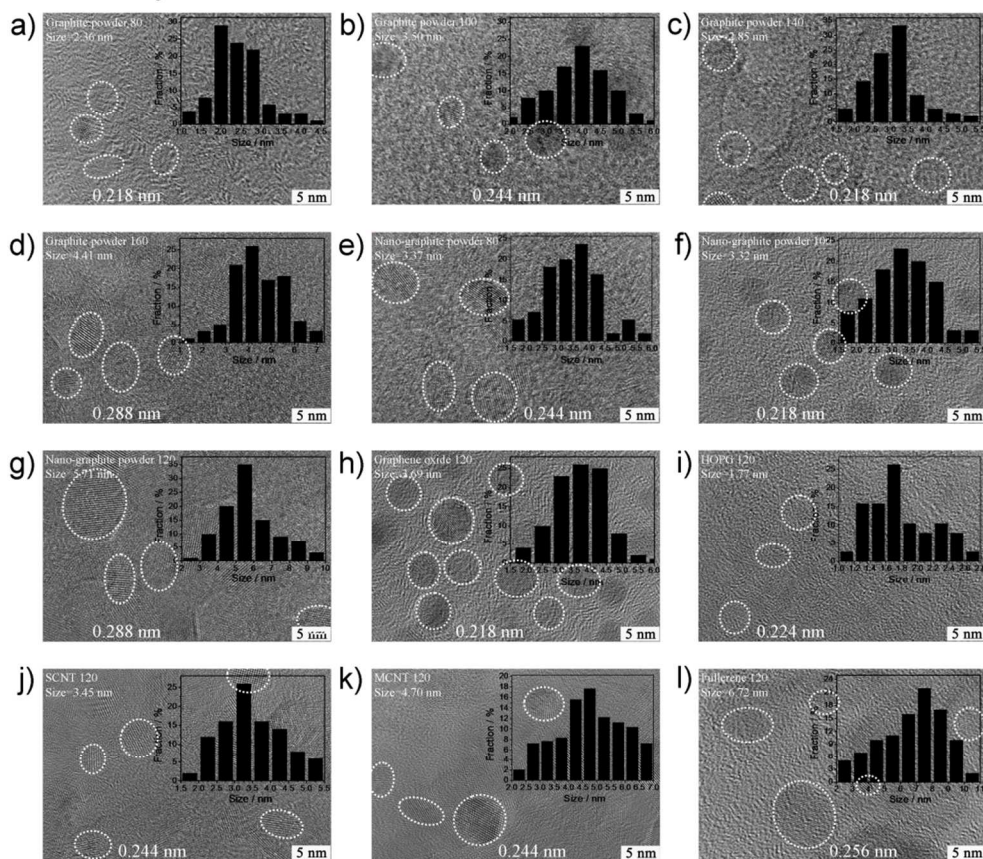
Fig. 4 The TEM image of GQDs prepared from different carbon resource: a) Graphite powder at 80 °C cutting, b) Graphite powder at 100 °C cutting,

c) Graphite powder at 140 °C cutting, d) Graphite powder at 160 °C cutting, e) Nano-graphite powder at 80 °C cutting, f) Nano-graphite powder at 100 °C cutting, g) Nano-graphite powder at 120 °C cutting, h) Graphene oxide at 80 °C cutting, i) Highly oriented pyrolytic graphite
5 (HOPG) at 120 °C cutting, j) Single wall carbon nanotube (SCNT) at 120 °C cutting, k) Multi wall carbon nanotube (MCNT) at 120 °C cutting, l) Fullerene at 80 °C cutting.

Due to the surface state PL of the GQDs, The PL properties can be improved by edge modifying, from Fig. 5a, using the one-
10 step solvothermal treatment of the GQDs by DMF and water as co-solvent,[47, 48] the m-GQDs were obtained with elevated quantum yield (4.7%, determined by absolute quantum yield measurement). The PL intensity of m-GQDs was higher than that of GQDs (Fig. S10) while the optimal excitation wavelength of
15 m-GQDs was blue shifted (400 nm excitation) compared with the initiative GQDs', and they can give bright green emission by handhold UV lamps (Fig. 5b-c). The lifetime of m-GQDs also increased at all wavelengths compared with GQDs (Fig. 5d), and the long lifetime (τ_2) referred to the radiative transition increased
20 a lot compared with that of GQDs (Table S3). From the TA spectra of m-GQDs, an obvious stimulated emission (SE) appeared (Fig. 5e), which was nearly the same as the common green PL center in other kinds of GQDs and carbon nanodots, but the SE signal was weaker than that of CDs with high quantum
25 yield (the higher PL quantum yield is, the more remarkable SE exhibits).[42] As a result, we deduced that the surface state was enhanced from GQDs to m-GQDs by changing partial carboxyl groups to amide based groups (the $-CON(CH_3)_2$ is the stronger green PL center than $-COOH$). It should be noted that the
30 nitrogen doped structures (Fig. S3) in the initiative GQDs were generally recognized to enhance the blue emission,[49-51] which was very different for the amide groups at the edge of the m-GQDs.
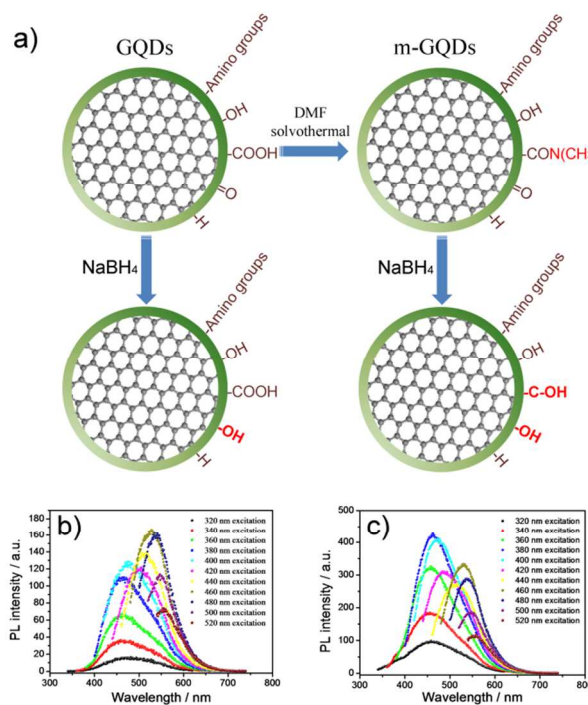
solutions. c) The PL excitation spetra of m-GQDs. Insets show photographs of m-GQDs in aqueous solutions under visible and UV light. d) The lifetime of the GQDs and m-GQDs at 375 nm excitation and probed at different wavelength sections. e) TA spectra of m-GQDs, there
40 was both a positive excited-state absorption (ESA) and negative stimulated emission (SE).

To further prove the surface state of the GQDs, we used $NaBH_4$ to reduce the GQDs and m-GQDs. The $NaBH_4$ selectively reduced the epoxy, carbonyl and amido (Fig. 6a), so the epoxy
45 groups were all removed from GQDs, m-GQDs to the reduced GQDs and m-GQDs. The different point is that the $-COOH$ can not be reduced while the $C=O$ and $-CON(CH_3)_2$ can be reduced to $-OH$. As a result, the reduced m-GQDs possessed more $-OH$ groups compared with the reduced GQDs, resulting more blue PL
50 center and elevated QYs for the reduced m-GQDs ($-OH$-based hybrid structure mainly contributed to the blue emission and also enriched the electron density of the π structure) (Fig. 6b-c).[52] It should be also noted that not all the amino could be converted to the $-OH$, so the green-surface state was also left in some degree
55 after reducing.

It should be noted that the initial GQDs also possessed epoxy in the plane of the graphene core, after DMF solvothermal or reducing treatment, the epoxy was removed. However, there were no any evidences to support the epoxy contributed to the green
60 emission in this study. The epoxy groups were always regarded to induce non-radiative recombination of localized electron-hole pairs and hold back the intrinsic state (blue) emission of GQDs.[12] As a result, removing epoxy groups can enhance the integration of π conjugated system of GQDs, resulting elevated PL emission.

Fig. 5 The optical property of m-GQDs. a) Synthesis of m-GQDs by the
35 DMF solvothermal of GQDs. b) The PL spectra of m-GQDs in aqueous

65 **Fig. 6** The $NaBH_4$ reduction of GQDs and m-GQDs. a) The scheme of GQDs, m-GQDs and their reduction. b-c) The PL spectra of reduced GQDs and m-GQDs, respectively.

3. Conclusion

In conclusion, a universal route to GQDs was developed based on the acid-assisted cutting methods. The PL center of the GQDs was suggested to be the surface state, which was formed by the hybridization structure of edge groups and the connected graphene core, and the efficient edge groups for green emission were mainly carboxyl and amide. It was proved by the following three cases: one is that the PL of GQDs was enhanced by the UV exposure, during which partial -OH of GQDs changed into carboxyl groups; the second one is the PL properties of GQDs can be further improved by one-step solvothermal treatment, in which partial carboxyl groups were changed to amide ones and the surface state of GQDs was enhanced; thirdly, the reduced m-GQDs possessed more -OH groups compared with the reduced GQDs, resulting more blue PL center. The quantum yield of the GQDs can be enhanced by three points: the elevated PL center by edge modifying; the enriched electron density of the π structure by reducing; the suppression of non-radiative recombination by removing the epoxy. The present work gave a deep investigation on the surface state of the GQDs, which is very important for understanding the PL mechanism of the related carbon based materials.

4. Experimental detail

4.1 Preparation of GQDs. 300 mg graphite powder (nano-graphite powder, graphene oxide, highly oriented pyrolytic graphite, single/multi wall carbon nanotube and fullerene) was dispersed in mixed acid (containing concentrated HNO_3 20 mL and concentrated H_2SO_4 60 mL). Then put the solution into a 100 mL round-bottom flask, stirred at 120 °C (80, 100, 140 and 160 °C was also used for investigating the universality of the present reaction) for 10 h. After the reaction, dilute the solution by pouring it into 300 mL di-water, followed by neutralizing the acid with Na_2CO_3. Concentrate and put the solution into the refrigerator to remove the Na_2SO_4 salt from the solution as much as possible (repeat three times). Aggregation in the solution was then excluded by filter membrane of 220 nm. Finally, 3500 dialysis bag was used to further purify the sample.

4.2 Preparation of m-GQDs. 9 mL DMF was added in 1 mL GQDs aqueous solution (0.1-1 mg/mL) and submitted to ultrasonication for 10 min. After that, the mix solution was put in the a 30 mL of Teflon lined autoclave, and kept heating at 200 °C for 5 hour. The obtained product was collected by rotary evaporation.

4.3 Characterization. High-resolution transmission electron microscope (HTEM) was recorded on JEOL JEM-2100F. Fluorescence spectroscopy was performed with a Shimadzu RF-5301 PC spectrophotometer. UV-vis absorption spectra were obtained using a Shimadzu 3100 UV-vis spectrophotometer. Nanosecond fuorescence lifetime experiments were performed using the time-correlated single-photon counting (TCSPC) system at right-angle sample geometry (F980). IR spectra were taken on a Nicolet AVATAR 360 FT-IR spectrophotometer. The confocal microscopy images were taken at Olympus Fluoview FV1000. X-ray Photoelectron Spectroscopy (XPS) was investigated by using ESCALAB 250 spectrometer with a mono X-Ray source Al Kα excitation (1486.6 eV). Binding energy calibration was based on C1s at 284.6 eV. AFM images were recorded in the tapping mode with a Nanoscope IIIa scanning probe microscope from Digital Instruments under ambient conditions. Matrix-assisted laser desorption/ionization reflect time-of-flight (MALDI-TOF) technique was recorded on Bruker autoflex speed TOF with tetracyanoquinodimethane (TCNQ) as the matrix. Zeta potential and DLS measurements were performed using a Zetasizer Nano-ZS (Malvern Instruments). Each sample was measured 5 times and the average data was presented. Absolute quantum yield was measured on fluorescence lifetime and steady state spectrometer (Edinburgh Instrument, FLS 920, with an integrating sphere).

4.4 Femtosecond transient absorption setup. The TA setup consisted of 400 nm pump pulses doubled from 800 nm laser pulses (~100 fs duration, 250 Hz repetition rate) generated from a mode-locked Ti: sapphire laser/amplifier system (Solstice, Spectra-Physics) and broadband white-light probe pulses generated from 2-mm-thick water. The TA data were collected by a fiber-coupled spectrometer connected to a computer. The group velocity dispersion of the transient spectra was compensated by a chirp program. All of the measurements were preformed at room temperature.

Acknowledgements

Notes and references

ᵃ State Key Laboratory of Supramolecular Structure and Materials, College of Chemistry, Jilin University, 2699 Qianjin Street, Changchun 130012, China
Email: byangchem@jlu.edu.cn
ᵇ State Key Laboratory on Integrated Optoelectronics, College of Electronic Science and Engineering, Jilin University
† Electronic Supplementary Information (ESI) available: Other structure characterizations, schemes, lifetime tables and optical measurements. See DOI: 10.1039/b000000x/

1. K. Welsher, Z. Liu, S. P. Sherlock, J. T. Robinson, Z. Chen, D. Daranciang and H. Dai, *Nature Nanotech.*, 2009, **4**, 773-780.
2. T. Gokus, R. R. Nair, A. Bonetti, M. Bohmler, A. Lombardo, K. S. Novoselov, A. K. Geim, A. C. Ferrari and A. Hartschuh, *ACS Nano*, 2009, **3**, 3963-3968.
3. S. N. Baker and G. A. Baker, *Angew. Chem. Int. Ed.*, 2010, **49**, 6726-6744.
4. H. Li, Z. Kang, Y. Liu and S.-T. Lee, *J. Mater. Chem.*, 2012, **22**, 24230-24253.
5. L. Cao, M. J. Meziani, S. Sahu and Y. P. Sun, *Acc. Chem. Res.*, 2013, **46**, 171-180.

6. S. Zhu, Y. Song, X. Zhao, J. Shao, J. Zhang and B. Yang, *Nano Res.*, 2015, **8**, 355-381.

7. D. Pan, J. Zhang, Z. Li and M. Wu, *Adv. Mater.*, 2010, **22**, 734-738.

8. Y. Li, Y. Hu, Y. Zhao, G. Shi, L. Deng, Y. Hou and L. Qu, *Adv. Mater.*, 2011, **23**, 776-780.

9. S. Zhu, J. Zhang, C. Qiao, S. Tang, Y. Li, W. Yuan, B. Li, L. Tian, F. Liu, R. Hu, H. Gao, H. Wei, H. Zhang, H. Sun and B. Yang, *Chem. Commun.*, 2011, **47**, 6858-6860.

10. L.-L. Li, J. Ji, R. Fei, C.-Z. Wang, Q. Lu, J.-R. Zhang, L.-P. Jiang and J.-J. Zhu, *Adv. Funct. Mater.*, 2012, **22**, 2971-2979.

11. K. Lingam, R. Podila, H. Qian, S. Serkiz and A. M. Rao, *Adv. Funct. Mater.*, 2013, **23**, 5062-5065.

12. S. Zhu, J. Zhang, S. Tang, C. Qiao, L. Wang, H. Wang, X. Liu, B. Li, Y. Li, W. Yu, X. Wang, H. Sun and B. Yang, *Adv. Funct. Mater.*, 2012, **22**, 4732-4740.

13. T. F. Yeh, C. Y. Teng, S. J. Chen and H. Teng, *Adv. Mater.*, 2014, **26**, 3297-3303.

14. C. F. Chen, C. H. Park, B. W. Boudouris, J. Horng, B. Geng, C. Girit, A. Zettl, M. F. Crommie, R. A. Segalman, S. G. Louie and F. Wang, *Nature*, 2011, **471**, 617-620.

15. R. Kim, V. Perebeinos and P. Avouris, *Physical Review B*, 2011, **84**.

16. D. B. Shinde and V. K. Pillai, *Angew. Chem. Int. Ed.*, 2013, **52**, 2482-2485.

17. S. Zhu, S. Tang, J. Zhang and B. Yang, *Chem. Commun.*, 2012, **48**, 4527-4539.

18. L. Tang, R. Ji, X. Li, K. S. Teng and S. P. Lau, *Part. Part. Syst. Charact.*, 2013, **30**, 523-531.

19. J. Shen, Y. Zhu, X. Yang and C. Li, *Chem. Commun.*, 2012, **48**, 3686-3699.

20. J. Peng, W. Gao, B. K. Gupta, Z. Liu, R. Romero-Aburto, L. Ge, L. Song, L. B. Alemany, X. Zhan, G. Gao, S. A. Vithayathil, B. A. Kaipparettu, A. A. Marti, T. Hayashi, J. J. Zhu and P. M. Ajayan, *Nano Lett.*, 2012, **12**, 844-849.

21. R. Ye, C. Xiang, J. Lin, Z. Peng, K. Huang, Z. Yan, N. P. Cook, E. L. Samuel, C. C. Hwang, G. Ruan, G. Ceriotti, A. R. Raji, A. A. Marti and J. M. Tour, *Nature Commun.*, 2013, **4**, 2943.

22. D. B. Shinde and V. K. Pillai, *Chem. Eur. J.*, 2012, **18**, 12522-12528.

23. T. S. Sreeprasad, A. A. Rodriguez, J. Colston, A. Graham, E. Shishkin, V. Pallem and V. Berry, *Nano Lett.*, 2013, **13**, 1757-1763.

24. P. Luo, Z. Ji, C. Li and G. Shi, *Nanoscale*, 2013, **5**, 7361-7367.

25. M. Hassan, E. Haque, K. R. Reddy, A. I. Minett, J. Chen and V. G. Gomes, *Nanoscale*, 2014, **6**, 11988-11994.

26. L. Lin and S. Zhang, *Chem. Commun.*, 2012, **48**, 10177-10179.

27. W.-W. Liu, Y.-Q. Feng, X.-B. Yan, J.-T. Chen and Q.-J. Xue, *Adv. Funct. Mater.*, 2013, **23**, 4111-4122.

28. H. Tetsuka, R. Asahi, A. Nagoya, K. Okamoto, I. Tajima, R. Ohta and A. Okamoto, *Adv. Mater.*, 2012, **24**, 5333-5338.

29. Y. Wang, S. Kalytchuk, Y. Zhang, H. Shi, S. V. Kershaw and A. L. Rogach, *J. Phys. Chem. Lett.*, 2014, **5**, 1412-1420.

30. Z. X. Gan, S. J. Xiong, X. L. Wu, C. Y. He, J. C. Shen and P. K. Chu, *Nano Lett.*, 2011, **11**, 3951-3956.

31. S. Chen, J. W. Liu, M. L. Chen, X. W. Chen and J. H. Wang, *Chem. Commun.*, 2012, **48**, 7637-7639.

32. L. Zhou, J. Geng and B. Liu, *Part. Part. Syst. Charact.*, 2013, **30**, 1086-1092.

33. S. K. Cushing, M. Li, F. Huang and N. Wu, *ACS Nano*, 2014, **8**, 1002-1013.

34. S. Zhu, L. Wang, B. Li, Y. Song, X. Zhao, G. Zhang, S. Zhang, S. Lu, J. Zhang, H. Wang, H. Sun and B. Yang, *Carbon*, 2014, **77**, 462-472.

35. F. Liu, M. H. Jang, H. D. Ha, J. H. Kim, Y. H. Cho and T. S. Seo, *Adv. Mater.*, 2013, **25**, 3657-3662.

36. S. Zhu, J. Zhang, L. Wang, Y. Song, G. Zhang, H. Wang and B. Yang, *Chem. Commun.*, 2012, **48**, 10889-10891.

37. S. Zhu, L. Wang, N. Zhou, X. Zhao, Y. Song, S. Maharjan, J. Zhang, L. Lu, H. Wang and B. Yang, *Chem. Commun.*, 2014, **50**, 13845-13848.

38. L. Wang, H. Y. Wang, Y. Wang, S. J. Zhu, Y. L. Zhang, J. H. Zhang, Q. D. Chen, W. Han, H. L. Xu, B. Yang and H. B. Sun, *Adv. Mater.*, 2013, **25**, 6539-6545.

39. L. Wang, S.-J. Zhu, H.-Y. Wang, Y.-F. Wang, Y.-W. Hao, J.-H. Zhang, Q.-D. Chen, Y.-L. Zhang, W. Han, B. Yang and H.-B. Sun, *Adv. Opt. Mater.*, 2013, **1**, 264-271.

40. S. H. Jin, H. Kim da, G. H. Jun, S. H. Hong and S. Jeon, *ACS Nano*, 2013, **7**, 1239-1245.

41. L. Wang, Y. Wang, T. Xu, H. Liao, C. Yao, Y. Liu, Z. Li, Z. Chen, D. Pan, L. Sun and M. Wu, *Nature Commun.*, 2014, **5**, 5357.

42. L. Wang, S. J. Zhu, H. Y. Wang, S. N. Qu, Y. L. Zhang, J. H. Zhang, Q. D. Chen, H. L. Xu, W. Han, B. Yang and H. B. Sun, *ACS Nano*, 2014, **8**, 2541-2547.

43. Y. Dong, J. Lin, Y. Chen, F. Fu, Y. Chi and G. Chen, *Nanoscale*, 2014, **6**, 7410-7415.

44. F. Jiang, D. Chen, R. Li, Y. Wang, G. Zhang, S. Li, J. Zheng, N. Huang, Y. Gu, C. Wang and C. Shu, *Nanoscale*, 2013, **5**, 1137-1142.

45. Y. Shin, J. Lee, J. Yang, J. Park, K. Lee, S. Kim, Y. Park and H. Lee, *Small*, 2014, **10**, 866-870.

46. L. Fan, Y. Hu, X. Wang, L. Zhang, F. Li, D. Han, Z. Li, Q. Zhang, Z. Wang and L. Niu, *Talanta*, 2012, **101**, 192-197.

47. S. Zhu, J. Zhang, X. Liu, B. Li, X. Wang, S. Tang, Q. Meng, Y. Li, C. Shi, R. Hu and B. Yang, *RSC Adv.*, 2012, **2**, 2717.

48. Q. Liu, B. Guo, Z. Rao, B. Zhang and J. R. Gong, *Nano Lett.*, 2013, **13**, 2436-2441.

49. X. Wang, F. Zhang, J. Liu, R. Tang, Y. Fu, D. Wu, Q. Xu, X. Zhuang, G. He and X. Feng, *Org. Lett.*, 2013, **15**, 5714-5717.

50. S. Yang, L. Zhi, K. Tang, X. Feng, J. Maier and K. Müllen, *Adv. Funct. Mater.*, 2012, **22**, 3634-3640.

51. G. S. Kumar, R. Roy, D. Sen, U. K. Ghorai, R. Thapa, N. Mazumder, S. Saha and K. K. Chattopadhyay, *Nanoscale*, 2014, **6**, 3384-3391.

52. A. Ananthanarayanan, X. W. Wang, P. Routh, B. Sana, S. Lim, D. H. Kim, K. H. Lim, J. Li and P. Chen, *Adv. Funct. Mater.*, 2014, **24**, 3021-3026.

Nanoscale Accepted Manuscript